

Article

## Three-Dimensional Structures Based on the Fusion of Chrysene and Spirobifluorene Chromophores for the Development of Blue OLEDs

Hayoon Lee, Hyecheol Jung, Seokwoo Kang, Jin Hyuck Heo, Sang Hyuk Im, and Jongwook Park

*J. Org. Chem.*, **Just Accepted Manuscript** • DOI: 10.1021/acs.joc.7b03008 • Publication Date (Web): 19 Feb 2018

Downloaded from <http://pubs.acs.org> on February 20, 2018

### Just Accepted

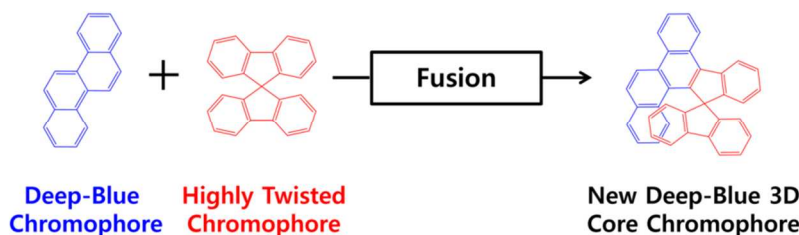
“Just Accepted” manuscripts have been peer-reviewed and accepted for publication. They are posted online prior to technical editing, formatting for publication and author proofing. The American Chemical Society provides “Just Accepted” as a service to the research community to expedite the dissemination of scientific material as soon as possible after acceptance. “Just Accepted” manuscripts appear in full in PDF format accompanied by an HTML abstract. “Just Accepted” manuscripts have been fully peer reviewed, but should not be considered the official version of record. They are citable by the Digital Object Identifier (DOI®). “Just Accepted” is an optional service offered to authors. Therefore, the “Just Accepted” Web site may not include all articles that will be published in the journal. After a manuscript is technically edited and formatted, it will be removed from the “Just Accepted” Web site and published as an ASAP article. Note that technical editing may introduce minor changes to the manuscript text and/or graphics which could affect content, and all legal disclaimers and ethical guidelines that apply to the journal pertain. ACS cannot be held responsible for errors or consequences arising from the use of information contained in these “Just Accepted” manuscripts.

# Three-Dimensional Structures Based on the Fusion of Chrysene and Spirobifluorene Chromophores for the Development of Blue OLEDs

Hayoon Lee<sup>†</sup>, Hyocheol Jung<sup>†</sup>, Seokwoo Kang<sup>†</sup>, Jin Hyuck Heo<sup>‡</sup>, Sang Hyuk Im<sup>‡</sup> and Jongwook Park<sup>†\*</sup>

<sup>†</sup> Department of Chemical Engineering, College of Engineering, Kyung Hee University (KHU), 1732 Deogyong-daero, Giheung, Youngin, Gyeonggi, 17104, Republic of Korea

<sup>‡</sup> Department of Chemical and Biological Engineering, Korea University, 145 Anam-ro, Seongbuk-gu, Seoul 136-713, Republic of Korea



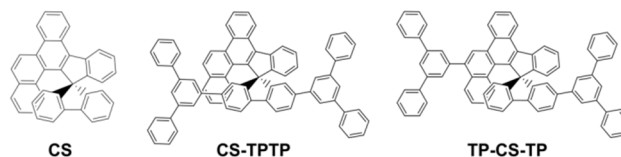
**ABSTRACT:** A new deep-blue chromophore containing a three-dimensionally (3D) shaped CS core composed of fused chrysene and spirofluorene units is synthesized. A pair of *m*-terphenyl (TP) units is also substituted onto the CS core, at two different sets of positions to form two additional compounds: CS-TPTP and TP-CS-TP. The TP-CS-TP compound showed the highest efficiency with an external quantum efficiency (EQE) of 3.05%, and Commission Internationale de L'Eclairage coordinates (CIE) of (0.148, 0.098) corresponding to the emission of blue light. This approach for forming a new chromophore is expected to the development of functional organic materials with excellent characteristics.

## INTRODUCTION

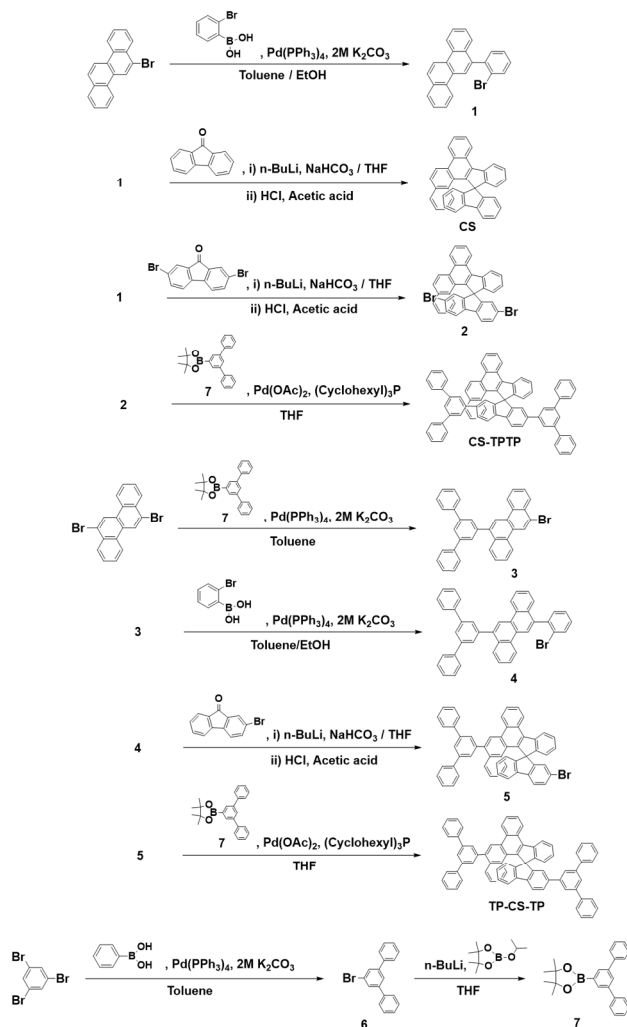
Many studies are underway to develop materials with high efficiency for various optoelectronic applications, such as organic light-emitting diodes (OLEDs), organic thin film transistors (OTFTs), and organic photovoltaics (OPVs).<sup>1-3</sup> By using the core-side concept of material development in these fields, it is possible to design and develop materials having the desired properties.<sup>4</sup>

In the case of OLEDs, the core group is responsible for the main absorption and emission roles of the final compound; and the side groups, which are capable of controlling the size, arrangement, polarity, etc., of the final molecule, are substituted onto the core to form compounds with a variety of shapes. In particular, the emission characteristics can be adjusted by changing the symmetry properties of the connections of the side groups to the core and changing the positions on the core at which the side groups are substituted.<sup>4</sup> We have also reported a systematic study of a core composed of single, dual, and triple chromophores, and the relationship between the final compound and the substituted side groups.<sup>5</sup> We used side groups with different sizes, such as *m*-terphenyl (TP) and triphenylbenzene (TPB), as well as different electron-donating effects, such as diphenylamine (DPA) and triphenylamine (TPA).<sup>5a,5d</sup>

In an OLED, the inclusion of materials that emit red, green, and blue light is essential to realize a full-color display. But materials that emit blue light have a wide energy band gap, which causes high barriers to the injection of charge into the device. Thus, the blue OLED devices developed so far are inferior to green and red OLEDs in terms of electroluminescence (EL) efficiency and device lifetime.<sup>6</sup> Therefore, development of materials that emit blue light with a pure color and high efficiency is still required. In particular, Commission Internationale de L'Eclairage coordinates (CIE *x*, *y*) of (0.14, 0.08) are required by the National Television System Committee (NTSC); and high-definition television (HDTV) ITU-R BT.709 requires a deeper-blue emission with CIE *x*, *y* of (0.15, 0.06).



**Scheme 1.** Chemical structures of the synthesized compounds.



**Scheme 2.** Synthetic routes of the synthesized materials.

Three approaches using the core-side concept mentioned above have been described for developing materials that emit deep-blue light. One approach involves the use of a core that emits deep-blue light as the chromophore, with anthracene, pyrene, chrysene, and fluorene being examples of such cores.<sup>7</sup> The second involves using a molecule with a highly twisted angle between its cores or between its core and side group in order to limit the extent of conjugation in the molecule.<sup>5b,8</sup> And the third approach entails using bulky side groups with relatively low inductive effects to sufficiently hinder intermolecular packing.<sup>5a,5d,7b</sup> So far, for deep-blue OLEDs, a chromophore mentioned above was selected as a single core and its derivatives were synthesized. However, since the number of chromophores that can be formed by a single core is limited, a new core preparation method that can provide a new chromophore compound is required.

In this study, we propose a fused system based on a three-dimensional (3D) shape between chromophores to design a new deep-blue chromophore using a single core. We synthesized a new core, spiro[fluorene-9,15'-indeno[2,1-g]chrysene] (CS); we designed this compound as a fusion of chrysene and spirobifluorene sharing a phenyl ring. Chrysene emits deep-blue light, compared to the emission of other chromophores such as anthracene and pyrene.<sup>7b</sup> Spirobifluorene also has the advantage of consisting of a highly-twisted fluorene that prevents an increased extent of conjugation and that maintains a

3D rather than planar shape.<sup>9</sup> A fusion of these two component chromophores into a single chromophore (rather than a simple coupling of the components using a carbon-carbon single bond) resulted in a product with increased rigidity, and hence a reduced rate of non-radiative relaxation.<sup>10</sup> We also used CS core to synthesize 2,7-di([1,1':3',1''-terphenyl]-5'-yl)spiro[fluorene-9,15'-indeno[2,1-g]chrysene] (CS-TPTP) and 2,5'-di([1,1':3',1''-terphenyl]-5'-yl)spiro[fluorene-9,15'-indeno[2,1-g]chrysene] (TP-CS-TP), and investigated the effect of the substitution position of the bulky TP side group on the emission wavelength and efficiency of the final molecule.

## RESULTS AND DISCUSSION

The chemical structures of the newly synthesized compounds are shown in scheme 1. They were synthesized using the well-known and generally simple Suzuki coupling, bromination, and borylation reactions, and the details of the synthesis methods used are described in the experimental section and scheme 2. The ultraviolet-visible (UV-Vis) absorption and photoluminescence (PL) spectra of the synthesized materials are shown in Figure 1. The optical properties, energy levels of the molecular orbitals, and thermal properties of these materials are summarized in Table 1.

In the solution state and film state, CS showed UV-Vis maximum (UV<sub>max</sub>) absorption peaks at wavelengths in the range of 360 nm to 387 nm. We also acquired UV spectra of chrysene and spirobifluorene; they showed, UV<sub>max</sub> absorption at wavelengths in the range of 250 nm to 321 nm, shorter than those of CS and expected since they are deep-blue chromophores (Figure S1). The dihedral angle at the  $\alpha$  position of the bifluorene portion of CS was calculated via density functional theory (DFT) at the B3LYP / 6-31G (d) level to be 110.5°. The C24 - C25 - C26 ( $\alpha$  position) angle was confirmed from the single crystal of CS to be 104.0°, similar to the calculated values and also indicative of the highly twisted structure (Figure 2, Figure S2, Table S1). Thus, CS still retained the UV-Vis absorption characteristics of chrysene and spirobifluorene in the short-wavelength region.<sup>5b,8</sup> In addition, the electron density of CS was found not to be preferentially distributed to one side or the other of the molecule, i.e., neither to the chrysene portion nor the bifluorene portion of the molecule, and in this manner CS displays a feature new for chromophores.

CS-TPTP in the solution state and the film state also showed UV<sub>max</sub> absorption peaks in the wavelength range of 344 nm to 389 nm, similar to the results for CS. We attributed this similarity to the conjugation of the CS moiety not extending to the two attached TP side groups as a result of the highly twisted nature of both fluorenes observed for CS. Moreover, the same level of electron density was indicated to be present in the CS moiety of CS-TPTP as in CS (i.e., without the substituted TPTP side groups), as shown in Figure 2.

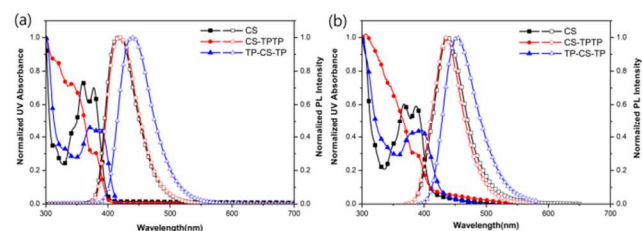


**Figure 1.** UV-Vis absorption and PL spectra of the synthesized materials: (a) in  $1 \times 10^{-5}$  M THF solution and (b) in vacuum-deposited films state.

**Table 1. Physical properties of the synthesized materials**

compd	$\lambda_{\max}$ abs (nm) solns <sup>a</sup> /films <sup>b</sup>		$\lambda_{\max}$ PL (nm) solns <sup>a</sup> /films <sup>b</sup>		$\Phi_f^c$	HOMO (eV) <sup>d</sup>	LUMO (eV) <sup>e</sup>	band gap (eV)	$t_g$ (°C)	$t_m$ (°C)	$t_d$ (°C) <sup>f</sup>
CS	360, 377	367, 387	417	436	0.61	-5.63	-2.59	3.04	108	250	358
CS-TPTP	344, 379	346, 389	420	436	0.59	-5.79	-2.77	3.02	195	-	522
TP-CS-TP	372, 387	377, 396	440	454	0.87	-5.70	-2.78	2.92	191	-	522

<sup>a</sup>Measured in  $1 \times 10^{-5}$  M THF solution. <sup>b</sup>Measured in 50 nm vacuum-deposited films. <sup>c</sup>Absolute PLQY in  $1 \times 10^{-5}$  M toluene solution. <sup>d</sup>Ultraviolet photoelectron spectroscopy (Riken-keiki, AC-2). <sup>e</sup>LUMO obtained from the HOMO and the optical band gap. <sup>f</sup>5% weight loss.

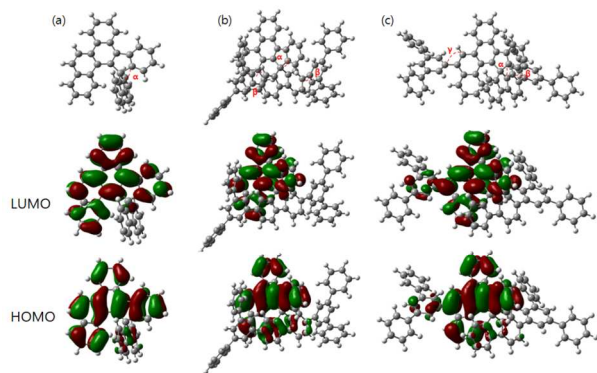


**Figure 2.** Optimized geometries and HOMO/LUMO electron density distributions of (a) CS, (b) CS-TPTP, and (c) TP-CS-TP.

TP-CS-TP exhibited  $UV_{\max}$  absorption peaks in the range of 372 nm to 396 nm, i.e., red-shifted approximately 10 nm compared to CS. This small difference was attributed to a small increase in the extent of the  $\pi$ -conjugation in TP-CS-TP to the TP side group substituted on the chrysene portion of the molecule. Electron density was indicated to be present in TP-CS-TP up to this TP side group.<sup>11</sup>

The UV-Vis absorption pattern in the solution and film states of the three synthesized materials showed relatively sharp absorption peaks for CS and TP-CS-TP, whereas CS-TPTP displayed a broad absorption peak. The sharpness of the absorption peaks of CS was attributed to the rigidity of the molecule, caused by the fusion of the chrysene and spirobifluorene subunits. And TP-CS-TP apparently maintained not only the rigidity in the CS moiety, but also the rigidity from the side group attached to the chrysene portion of the molecule. However, the broadness of the absorption peak of CS-TPTP was attributed to it having two side groups attached to the fluorene portion, which apparently caused a decreased rigidity compared to CS and TP-CS-TP.<sup>10b,12</sup>

This rigidity result was explained by comparing the DFT-calculated torsion angles for the connections of the CS moiety to the TP side groups. Those on the fluorene ( $\beta$  position) and chrysene ( $\gamma$  position) portions of the CS moiety were calculated to be  $37^\circ$  and  $54^\circ$ , respectively. The greater dihedral angle for the connection to the chrysene portion would appear to explain the relatively high rigidity of TP-CS-TP, which includes such a connection, and the decreased rigidity of CS-TPTP, whose TP side groups only connect to the fluorene portion.

In the solution state, the PL maximum ( $PL_{\max}$ ) value of CS was observed at a wavelength of 417 nm, and that of CS-TPTP was similar, at 420 nm, but the  $PL_{\max}$  of TP-CS-TP was shown to be at 440 nm. In the film state,  $PL_{\max}$  values of CS

and CS-TPTP were both at 436 nm and that of TP-CS-TP was shown to be at 454 nm. The red shift of the  $PL_{\max}$  of TP-CS-TP compared to those of the other compounds was consistent with the electron density distributions described above, where no obvious difference was observed between the electron density distributions of CS-TPTP and CS, but for TP-CS-TP, the  $\pi$ -conjugation length was extended due to the side group substituted on the chrysene portion of the molecule (Figure 2).

The red shifts of the  $PL_{\max}$  values in the film state relative to those in the solution state were attributed to a decreased distance and hence formation of  $\pi$ - $\pi$  interactions between molecules in the film state. The somewhat smaller solution-to-film red shifts of  $PL_{\max}$  observed for CS-TPTP and TP-CS-TP, i.e., 16 nm and 14 nm, respectively, than for CS, i.e., 19 nm, were attributed to the intermolecular packing having been more effectively prevented by the substituted side groups of CS-TPTP and TP-CS-TP. Also, all three synthesized materials have CS, which is a 3D structure based on fusion of chrysene with the highly-twisted spirobifluorene, and an excimer was not expected to be generated in their film state.<sup>13</sup>

The absolute PL quantum yield (PLQY,  $\Phi_f$ ) values of CS and CS-TPTP were measured to be 61% and 59%, respectively. The substitution of the side groups only on the fluorene portion of the CS moiety was thought to slightly reduce the efficiency of CS by generating non-radiative decay caused by the rotation and vibration of the molecule. In contrast, the PLQY of TP-CS-TP was 87%, i.e., higher than that of CS by approximately 43%. We attributed this increase in PLQY to an increase in electron density of the CS moiety resulting from the substitution of the TP side group on the chrysene portion of the moiety; these results were also attributed to their EL properties.<sup>14</sup>

The radiative ( $k_{\text{rad}}$ ) and non-radiative rate constants ( $k_{\text{nr}}$ ) of the three synthesized compounds were calculated based on the results of fluorescence lifetime measurements. The fluorescence lifetime of CS, CS-TPTP and TP-CS-TP was 3.14, 3.07, and 2.14 ns, respectively. TP-CS-TP showed faster decay compared to CS and CS-TPTP. It could be explained by that TP-CS-TP has relatively weak intermolecular interaction compared to other two compounds. CS and CS-TPTP showed the same  $k_{\text{rad}}$  of  $1.94 \times 10^8$  /s and  $k_{\text{nr}}$  of  $12.3 \times 10^7$  /s and  $13.1 \times 10^7$  /s, respectively. However, TP-CS-TP showed the highest  $k_{\text{rad}}$  of  $4.09 \times 10^8$  /s and the lowest  $k_{\text{nr}}$  of  $5.80 \times 10^7$  /s. Thus, the value of  $k_{\text{rad}}/k_{\text{nr}}$  for TP-CS-TP was 7.04, which is the largest value among the three compounds. As a result, the trend in  $k_{\text{rad}}/k_{\text{nr}}$  among the three compounds was same as that for fluorescence quantum efficiency (Figure S3, Table S2).

The highest occupied molecular orbital (HOMO) levels of the three synthesized materials were determined to be -5.63 eV to -5.79 eV and the lowest unoccupied molecular orbital (LUMO) levels were from -2.59 eV to -2.78 eV. The electro-

chemical properties of the three compounds were measured by cyclic voltammetry (CV). All three compounds showed the first oxida

**Table 2. EL Performance of Synthesized Compounds**

compd	C.E. (cd/A) <sup>a</sup>	P.E. (lm/W) <sup>a</sup>	EQE (%) <sup>a</sup>	CIE (x,y) <sup>a</sup>	EL <sub>max</sub> (nm) <sup>b</sup>
CS	1.21	0.70	3.01	(0.153, 0.050)	435
CS-TPTP	0.84	0.44	2.12	(0.154, 0.049)	435
TP-CS-TP	2.39	1.19	3.05	(0.148, 0.098)	453

<sup>a</sup>Measured at 10 mA/cm<sup>2</sup>. <sup>b</sup>Measured at 7 V.

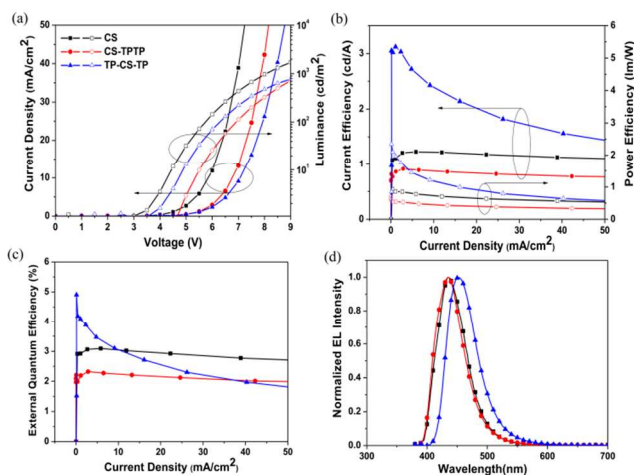


**Figure 3.** EL performances of the synthesized materials. (a) Current density-voltage-luminance characteristics. (b) Current and power efficiency as a function of current density at 10 mA/cm<sup>2</sup>. (c) External quantum efficiency as a function of current density at 10 mA/cm<sup>2</sup>. (d) EL spectra at 7 V.

-tion at around 1.0 V. After 30 CV cycles, the current intensity shapes were maintained for all three compounds, indicating that the compounds exhibited electrochemical stability for up to 30 cycles (Figure S4).

The decomposition temperature ( $t_d$ ) values of CS, CS-TPTP, and TP-CS-TP were measured to be 358 °C, 522 °C, and 522 °C, respectively. Generally, the larger the molecular weight, the larger the  $t_d$  value; hence, the essentially identical  $t_d$  values of CS-TPTP and TP-CS-TP were attributed to their identical molecular weights, and their  $t_d$  values being larger than that of CS was attributed to their greater molecular weights due to the substituted side groups (Figure S5(a)).

CS, CS-TPTP, and TP-CS-TP were measured to have glass transition temperature ( $t_g$ ) values of 108 °C, 195 °C, and 191 °C, respectively. This result was indicative of their high thermal stabilities. This result was also consistent with the 3D nature of the chemical structure promoting the formation of an amorphous state.<sup>15</sup> Using a chromophore with such a high thermal stability has been proposed to be important for forming a stable OLED device whose morphology does not easily change in the presence of the heat generated from the operation of the device.<sup>16</sup>

The melting temperature ( $t_m$ ) value of CS was measured at 250 °C, but the  $t_m$  values of CS-TPTP and TP-CS-TP were not obtained. This indicated that CS-TPTP and TP-CS-TP became more amorphous than CS, due to the TP side groups (Figure S5(b)). Thus, although a single crystal could be easily ob-

tained for CS as shown in Figure S1, single crystals could not be obtained for CS-TPTP and TP-CS-TP.

The synthesized compounds were used as non-doped emit-

ting layers (EMLs) in OLEDs with the following structure: ITO/NPB (40 nm)/TCTA (20 nm)/EML (30 nm)/TPBi (20 nm)/LiF (1 nm)/Al (200 nm). The OLED properties are summarized in Table 2 and Figure 3. CS showed a current efficiency (C.E.) of 1.21 cd/A, power efficiency (P.E.) of 0.70 lm/W, and external quantum efficiency (EQE) of 3.01%; it also showed a CIE of (0.153, 0.050) and EL maximum (EL<sub>max</sub>) value of 435 nm, indicative of emission in the deep-blue region. CS-TPTP showed a C.E. of 0.84 cd/A, P.E. of 0.44 lm/W, and EQE of 2.12%, approximately 30% lower than that of CS. As described above, CS-TPTP might undergo many occurrences of non-radiative decay caused by rotation and vibration of the side group and promoted by the relatively small approximately 37 ° dihedral angle of each of the two bonds connecting its core and side groups. Instead, CS-TPTP presumably has not only the highly twisted core structure of CS but also the lack of any extended  $\pi$ -conjugation. CS-TPTP showed a CIE of (0.154, 0.049) and EL<sub>max</sub> of 435 nm, very similar to those of CS and also indicative of emission in the deep-blue region.<sup>14</sup>

Of the three synthesized materials, TP-CS-TP showed the highest EL efficiency, with a C.E. of 2.39 cd/A, P.E. of 1.19 lm/W, and EQE of 3.05%. This current efficiency value was twice that of the CS core compound. This result was due to the high PLQY and can be also explained by the side group connected to the chrysene portion enriching the electron density of the CS moiety. TP-CS-TP, however, showed a CIE of (0.148, 0.098) and EL<sub>max</sub> of 453 nm, i.e., red-shifted by 18 nm that from CS. This difference was attributed to the intramolecularly lengthened  $\pi$ -conjugation of TP-CS-TP. The CIE and EL<sub>max</sub> values of TP-CS-TP were nevertheless still in the blue region.<sup>14</sup>

According to the increased current density of TP-CS-TP, the efficiency of this compound was decreased compared to those of CS and CS-TPTP. TP-CS-TP had a higher operating voltage than did CS or CS-TPTP (Figure 3(a)). However, considering the band diagram (Figure S6), charge injection is expected to be similar for the three compounds. This means that it is relatively difficult for TP-CS-TP to transport charge in the emitter compared to CS and CS-TPTP. To confirm carrier-transport properties of synthesized materials, hole only device (HOD) and electron only devices (EOD) were fabricated. The configuration of HOD and EOD were ITO/NPB (40 nm)/TCTA (20 nm)/EML (30nm)/NPB (20 nm)/Al (100 nm) and ITO/TPBi (40 nm)/EML (30nm)/TPBi (20 nm)/LiF (1 nm)/Al (100 nm), respectively. As shown in HOD and EOD data of Figure S7, the hole transporting property of three synthesized materials was similar but the electron transporting property of TP-CS-TP was slightly inferior to those of CS and CS-TPTP. Thus, TP-CS-TP might give rise to significant efficiency decay at high current density.<sup>17</sup>

## CONCLUSION

In this study, chrysene and spirobifluorene were fused, and a new deep-blue core chromophore, CS, having structural components extending in three dimensions, was synthesized. Also, in order to increase the efficiency or adjust the emission wavelength of the chromophore, we tested two additional compounds in which TP side groups were substituted at two different sets of positions of the CS core. In one of these compounds, i.e., TP-CS-TP, resulted in the highest current efficiency (with a value of 2.39 cd/A) and EQE (3.05%) of the three compounds synthesized. We expect this fused system to be used in future studies with other deep blue chromophores, such as anthracene, carbazole, and phenanthrene, to develop many additional new deep-blue 3D core chromophores. We also expect various novel blue luminescent materials to be made by systematically testing replacing the side group. This approach should lead to the development of organic functional materials with outstanding characteristics.

## EXPERIMENTAL SECTION

**General Methods.** The  $^1\text{H}$  NMR spectra and  $^{13}\text{C}$  NMR spectra were recorded on Bruker Avance 300 and Avance 500 spectrometers. The FAB+-mass was recorded on a JEOL, JMS-AX505WA, HP5890 series II. The optical absorption spectra were obtained by using a Lambda 1050 UV/Vis/NIR spectrometer (PerkinElmer). A PerkinElmer luminescence spectrometer LS55 (Xenon flash tube) was used to perform photoluminescence (PL) spectroscopy. Absolute PL quantum yield was measured using a JASCO FP8500 spectrometer in the toluene solution state. Time-resolved PL was estimated by Quantaurus-Tau fluorescence lifetime measurement system (C11367-03, Hamamatsu Photonics Co.) in toluene solution state. Cyclic voltammetry (CV) was performed on an AUTOLAB/PG-STAT12 model system with a three-electrode cell in a 0.1 M of tetrabutylammonium hexafluorophosphate (TBAHFP) and 1 mM of sample in acetonitrile at a scan rate of 100 mV/s. The glass transition temperatures ( $t_g$ ) and melting temperatures ( $t_m$ ) of the compounds were determined using differential scanning calorimetry (DSC) under a nitrogen atmosphere by using a DSC 4000 (PerkinElmer). Samples were heated from room temperature to 300 °C or 450 °C at a rate of 10 °C/min and cooled at 10 °C/min, then heated again under the same heating conditions as used in the initial heating process. Degradation temperatures ( $t_d$ ) were determined with thermogravimetric analysis (TGA) by using a TGA 4000 (PerkinElmer). Samples were heated from room temperature to 800 °C at a rate of 10 °C/min. The highest occupied molecular orbital (HOMO) levels of the synthesized materials were determined via photoelectron spectroscopy (Riken Keiki AC-2) by using an ultraviolet light energy source. The lowest unoccupied molecular orbital (LUMO) energy levels were calculated from the HOMO levels and the optical band gaps. The optical band gaps were derived by determining the absorption edges from plots of  $(h\nu)$  vs.  $(\alpha h\nu)^2$ , where  $\alpha$ ,  $h$ , and  $\nu$  are the absorbance, Planck's constant, and the frequency of light, respectively.

**Computational details.** We determined the optimized structures by using density functional theory (DFT) B3LYP/6-31G(d) calculations performed using the Gaussian09 program.<sup>18</sup> All of the optimized structures were characterized to be energy minima of the potential surfaces. Imaginary fre-

quencies were not found. Geometry optimization in Cartesian coordinates was shown in Table S3.

**Fabricated OLED device.** In each of the EL devices, N,N'-bis(naphthalen-1-yl)-N,N'-bis(phenyl)benzidine (NPB) was used for the hole injection layer (HIL), tris(4-carbazoyl-9-ylphenyl)amine (TCTA) was used for the hole transporting layer (HTL), one of the synthetic materials (CS, CS-TPTP, or TP-CS-TP) was used as the emitting layer (EML), 1,3,5-tris(1-phenyl-1H-benzimidazol-2-yl)benzene (TPBi) was used for the electron transporting layer (ETL), lithium fluoride (LiF) was used for the electron injection layer (EIL), ITO was used as the anode, and Al was used as the cathode. All organic layers were deposited under  $10^{-6}$  Torr, with a rate of deposition of 1 Å/s to create an emitting area of 4 mm<sup>2</sup>. The LiF and Al layers were continuously deposited under the same vacuum conditions. The luminance efficiency data for the fabricated EL devices were obtained by using a Keithley 2410 source meter. Light intensities were obtained using a Minolta CS-1000A spectroradiometer. The operational stabilities of the devices were measured under encapsulation in a glove box.

**Single crystal X-ray diffraction data of CS.** Each good quality air stable single crystal was mounted on a Bruker SMART CCD diffractometer. Diffraction data were collected at room temperature using graphite monochromated Mo K $\alpha$  radiation ( $k = 0.71073$  Å). The structure was solved by applying the direct method using SHELXS-97 and refined by a full-matrix least-squares calculation on F2 using SHELXL-97.<sup>19</sup> All non-H atoms were refined with anisotropic displacement parameters. Hydrogen atoms were fixed at ideal geometric positions, and their contributions were included in the structural factor calculations. The crystal data were as follows: C<sub>37</sub>H<sub>22</sub>; FW = 466.54, crystal size 0.30 × 0.29 × 0.27 mm<sup>3</sup>, Triclinic, P-1,  $a = 11.082(4)$  Å,  $b = 11.456(4)$  Å,  $c = 11.777(4)$  Å,  $\alpha = 92.038(19)^\circ$ ,  $\beta = 110.429(19)^\circ$ ,  $\gamma = 118.082(16)^\circ$ ,  $V = 1199.5(7)$  Å<sup>3</sup>,  $Z = 2$ ,  $D_c = 1.292$  mg/m<sup>3</sup>. The refinement converged to  $R_1 = 0.0514$ ,  $wR_2 = 0.1300$  ( $I > 2\sigma(I)$ ). CCDC 1557124.

**Synthesis.** 6-bromochrysene and 6,12-dibromo-chrysene were purchased from WITHCHEM co., Ltd. Compd **6** and **7** were synthesized according to the literature.<sup>20</sup>

**6-(2-Bromo-phenyl)-chrysene (1).** 6-bromochrysene (4.0 g, 1.30 mmol) and Pd(PPh<sub>3</sub>)<sub>4</sub> (0.76 g, 0.65 mmol) were added to anhydrous toluene solution (200 mL) under nitrogen. Then, 2-bromo-phenyl boronic acid (4.0 g, 2.00 mmol), which was dissolved in anhydrous ethanol (20 mL), was dropped slowly and 2 M K<sub>2</sub>CO<sub>3</sub> solution (100 mL) dissolved in H<sub>2</sub>O was added to the reaction mixture at 50 °C. The mixture was refluxed for 1 hour. After the reaction was complete, the reaction mixture was extracted with chloroform and water. The organic layer was dried with anhydrous MgSO<sub>4</sub> and filtered. The solution was evaporated. The product was isolated with silica gel column chromatography using toluene : n-hexane (1:10) as the eluent to obtain a white solid (1.5 g, 35%).  $^1\text{H}$  NMR (300 MHz, [D<sub>8</sub>]THF):  $\delta = 8.96$  (d, 1H), 8.88 (dd, 2H), 8.70 (s, 1H), 8.08 (d, 1H), 8.02 (d, 1H), 7.83 (d, 1H), 7.72-7.50 (m, 7H), 7.44 (m, 1H);  $^{13}\text{C}$  NMR (75 MHz, [D<sub>8</sub>]THF):  $\delta = 143.1$ , 139.5, 133.8, 133.6, 133.3, 131.9, 131.8, 130.4, 129.5, 129.4, 128.8, 128.6, 128.5, 127.7, 127.6, 127.4, 127.4, 125.5, 124.5, 124.4, 123.5, 122.1. HRMS (FAB/magnetic sector)  $m/z$ : [M]<sup>+</sup> Calcd. for C<sub>24</sub>H<sub>15</sub>Br 382.0357; Found 382.0359.

**Spiro[fluorene-9,15'-indeno[2,1-g]chrysenes] (CS).** Compd 1 (1.0 g, 2.61 mmol) was added to anhydrous THF solution (20 mL) under nitrogen. Then, 2.0 M n-butyllithium in cyclohexane (1.56 mL) was added slowly at -78 °C. Next, 9-fluorenone (0.56 g, 3.13 mmol) dissolved in anhydrous THF (10 mL) was added to the reaction mixture, followed by saturated NaHCO<sub>3</sub> solution (15 mL) at room temperature. The mixture was stirred for 3 h. After the reaction was complete, the reaction mixture was extracted with chloroform and water. The organic layer was dried with anhydrous MgSO<sub>4</sub> and filtered. The mixture was resolved acetic acid (50 mL) and 35 wt% HCl (5 mL) was added. The mixture was refluxed for 1 h. After the reaction was complete, the reaction mixture was extracted with chloroform and water. The organic layer was dried with anhydrous MgSO<sub>4</sub> and filtered. The solution was evaporated. The product was isolated with silica gel column chromatography using chloroform : n-hexane (1:2) as the eluent to obtain a white solid (0.49 g, 45%). <sup>1</sup>H NMR (300 MHz, [D<sub>8</sub>]THF): δ= 9.19 (d, 1H), 9.00 (d, 1H), 8.83 (d, 1H), 8.52 (d, 1H), 8.10 (d, 2H), 7.89-7.82 (m, 3H), 7.67 (d, 1H), 7.61 (d, 1H), 7.36-7.25 (m, 3H), 7.17 (t, 1H), 6.96-6.89 (m, 3H), 6.66 (d, 2H), 6.63 (t, 1H), 6.43 (d, 1H); <sup>13</sup>C NMR (75 MHz, [D<sub>8</sub>]THF): δ= 152.8, 149.5, 143.1, 141.2, 141.0, 133.9, 133.2, 131.2, 130.6, 129.5, 129.2, 128.9, 128.7, 128.6, 128.0, 127.9, 127.9, 127.8, 127.7, 126.5, 125.7, 125.5, 124.5, 124.1, 123.9, 123.7, 122.9, 121.7. HRMS (FAB/magnetic sector) m/z: [M]<sup>+</sup> Calcd. for C<sub>37</sub>H<sub>22</sub> 466.1722; Found, 466.1723. Anal. Calcd. for C<sub>37</sub>H<sub>22</sub>: C 95.25, H 4.75; Found: C 95.07, H 4.73.

**2,7-Dibromospiro[fluorene-9,15'-indeno[2,1-g]chrysenes]** (2). This compound was synthesized with the same method as for CS by using 2,7-dibromo-9-fluorenone (1.05 g, 3.13 mmol). Accordingly, a white solid was obtained (0.70 g, 47%). <sup>1</sup>H NMR (300 MHz, [D<sub>8</sub>]THF): δ= 9.20 (d, 1H), 9.04 (d, 1H), 8.88 (d, 1H), 8.57 (d, 1H), 8.07 (d, 2H), 7.94-7.84 (m, 3H), 7.76 (d, 1H), 7.56 (t, 3H), 7.37 (t, 1H), 7.25 (t, 1H), 7.03 (t, 1H), 6.82 (s, 2H), 6.66 (t, 1H), 6.44 (d, 1H); <sup>13</sup>C NMR (75 MHz, [D<sub>8</sub>]THF): δ= 151.7, 151.0, 141.2, 141.1, 139.4, 134.0, 133.4, 132.3, 131.5, 130.4, 129.4, 128.9, 128.5, 128.4, 128.3, 128.2, 126.8, 126.7, 125.8, 125.6, 124.8, 124.6, 123.6, 123.6, 123.2, 123.1. HRMS (FAB/magnetic sector) m/z: [M]<sup>+</sup> Calcd. for C<sub>37</sub>H<sub>20</sub>Br<sub>2</sub>, 621.9932; Found 621.9930.

**2,7-Di([1,1':3',1''-terphenyl]-5'-yl)spiro[fluorene-9,15'-indeno[2,1-g]chrysenes] (CS-TPTP).** Compd 2 (0.6 g, 0.96 mmol), compd 7 (0.82 g, 2.30 mmol), Pd(OAc)<sub>2</sub> (0.017 g, 0.075 mmol), and tricyclohexylphosphine (0.044 g, 0.16 mmol) were added to anhydrous THF (100 mL). Then, (Et)<sub>4</sub>NOH (20 wt%, 10 mL) was added to the reaction mixture at 50 °C. The mixture was refluxed for 3 h under nitrogen. After the reaction was complete, the reaction mixture was extracted with chloroform and water. The organic layer was dried with anhydrous MgSO<sub>4</sub> and filtered. The solution was evaporated. The product was isolated with silica gel column chromatography using chloroform : n-hexane (1:3) as the eluent to obtain a white solid (0.48 g, 60%). <sup>1</sup>H NMR (500 MHz, [D<sub>8</sub>]THF): δ= 9.15 (d, 1H), 9.00 (d, 1H), 8.84 (d, 1H), 8.50 (d, 1H), 8.28 (d, 2H), 7.92 (d, 1H), 7.83-7.77 (m, 5H), 7.70 (d, 1H), 7.64 (s, 2H), 7.55 (d, 8H), 7.42 (s, 4H), 7.34 (t, 8H), 7.32-7.23 (m, 5H), 7.20 (t, 1H), 7.02 (s, 2H), 6.98 (t, 1H), 6.68 (t, 1H), 6.62 (d, 1H); <sup>13</sup>C NMR (125 MHz, [D<sub>8</sub>]THF): δ= 152.6, 150.9, 143.2, 143.1, 142.5, 142.3, 142.1, 141.3, 141.3, 141.2, 133.8, 133.3, 131.3, 130.9, 129.6, 129.5, 129.4, 129.3, 128.5, 128.5, 128.2,

128.1, 128.0, 127.9, 127.9, 127.8, 126.7, 125.9, 125.8, 125.7, 125.5, 124.7, 124.2, 123.9, 123.1, 122.5, 122.2. HRMS (FAB/magnetic sector) m/z: [M+H]<sup>+</sup> Calcd. for C<sub>73</sub>H<sub>47</sub>, 923.3633; Found, 923.3635. Anal. Calcd. for C<sub>73</sub>H<sub>46</sub>: C 94.98, H 5.02; Found: C 94.75, H 5.07.

**6-Bromo-12-[1,1';3',1'']terphenyl-5'-yl-chrysenes (3).** 6,12-dibromo-chrysenes (4.0 g, 10.4 mmol), compd 7 (4.08 g, 11.5 mmol), and Pd(PPh<sub>3</sub>)<sub>4</sub> (0.48 g, 0.42 mmol) were added to anhydrous toluene solution (500 mL) under nitrogen. Then, 2 M K<sub>2</sub>CO<sub>3</sub> solution (50 mL) dissolved in H<sub>2</sub>O was added to the reaction mixture at 50 °C. The mixture was refluxed for 3 h. After the reaction was complete, the reaction mixture was extracted with chloroform and water. The organic layer was dried with anhydrous MgSO<sub>4</sub> and filtered. The solution was evaporated. The product was isolated with silica gel column chromatography using chloroform : n-hexane (1:10) as the eluent to obtain a white solid (2.5 g, 49%). <sup>1</sup>H NMR (300 MHz, [D<sub>8</sub>]THF): δ= 9.26 (s, 1H), 9.02-8.97 (m, 2H), 8.87 (s, 1H), 8.46-8.42 (m, 1H), 8.16 (d, 1H), 8.06 (s, 1H), 7.90 (s, 2H), 7.84-7.73 (m, 7H), 7.65 (t, 1H), 7.49 (t, 4H), 7.38 (t, 2H); <sup>13</sup>C NMR (75 MHz, [D<sub>8</sub>]THF): δ= 143.2, 143.1, 142.0, 141.1, 132.9, 132.4, 131.8, 131.3, 129.8, 129.5, 128.8, 128.8, 128.6, 128.5, 128.3, 128.0, 127.9, 126.6, 126.0, 125.1, 124.7, 123.5, 123.2. HRMS (FAB/magnetic sector) m/z: [M]<sup>+</sup> Calcd. for C<sub>36</sub>H<sub>23</sub>Br, 534.0983; Found 534.0984.

**6-(2-Bromo-phenyl)-12-[1,1';3',1'']terphenyl-5'-yl-chrysenes (4).** Compd 3 (5.0 g, 9.34 mmol) and Pd(PPh<sub>3</sub>)<sub>4</sub> (0.48 g, 0.42 mmol) were added to anhydrous toluene solution (200 mL) under nitrogen. Then, 2-bromo-phenyl boronic acid (2.3 g, 11.5 mmol), which was dissolved in anhydrous ethanol (20 mL), was dropped slowly and 2 M K<sub>2</sub>CO<sub>3</sub> solution (20 mL) dissolved in H<sub>2</sub>O was added to the reaction mixture at 50 °C. The mixture was refluxed for 30 min. After the reaction was complete, the reaction mixture was extracted with chloroform and water. The organic layer was dried with anhydrous MgSO<sub>4</sub> and filtered. The solution was evaporated. The product was isolated with silica gel column chromatography using toluene : n-hexane (1:10) as the eluent to obtain a white solid (1.1 g, 30%). <sup>1</sup>H NMR (300 MHz, [D<sub>8</sub>]THF): δ= 9.04 (d, 1H), 8.99 (d, 1H), 8.94 (s, 1H), 8.77 (s, 1H), 8.17 (d, 1H), 8.07 (s, 1H), 7.93 (d, 2H), 7.85 (d, 5H), 7.71-7.33 (m, 14H); <sup>13</sup>C NMR (75 MHz, [D<sub>8</sub>]THF): δ= 143.5, 143.1, 143.1, 142.1, 140.7, 139.6, 133.8, 132.3, 132.3, 132.0, 131.9, 130.5, 129.8, 128.9, 128.5, 128.3, 127.8, 127.7, 127.6, 127.6, 127.5, 125.9, 125.6, 124.8, 123.4, 123.4. HRMS (FAB/magnetic sector) m/z: [M]<sup>+</sup> Calcd. for C<sub>42</sub>H<sub>27</sub>Br, 610.1296; found 610.1288.

**5'-([1,1':3',1''-Terphenyl]-5'-yl)-2-bromospiro[fluorene-9,15'-indeno[2,1-g]chrysenes] (5).** Compd 4 (1.0 g, 1.64 mmol) was added to anhydrous THF solution (20 mL) under nitrogen. Then, 2.0 M n-butyllithium in cyclohexane (0.98 mL) was added slowly at -78 °C. Next, 2-bromo-9-fluorenone (0.51 g, 1.95 mmol) dissolved in anhydrous THF (10 mL) was added to the reaction mixture, followed by saturated NaHCO<sub>3</sub> solution (15 mL) at room temperature. The mixture was stirred for 3 h. After the reaction was complete, the reaction mixture was extracted with chloroform and water. The organic layer was dried with anhydrous MgSO<sub>4</sub> and filtered. The mixture was resolved in acetic acid (50 mL) and 35 wt% HCl (5 mL) was added. The mixture was refluxed for 1 h. After the reaction was complete, the reaction mixture was extracted with chloroform and water. The organic layer was dried with anhydrous

MgSO<sub>4</sub> and filtered. The solution was evaporated. The product was isolated with silica gel column chromatography using chloroform : n-hexane (1:2) as the eluent to obtain a white solid (0.48 g, 43%). <sup>1</sup>H NMR (300 MHz, [D<sub>8</sub>]THF): δ= 9.22 (d, 1H), 9.10 (d, 1H), 8.92 (s, 1H), 8.57 (d, 1H), 8.14 (d, 1H), 8.09 (d, 1H), 8.01 (s, 1H), 7.91-7.78 (m, 9H), 7.70 (d, 1H), 7.58 (dd, 1H), 7.47-7.31 (m, 8H), 7.16 (t, 1H), 7.02 (t, 2H), 6.94 (s, 1H), 6.69-6.60 (m, 2H), 6.45 (d, 1H); <sup>13</sup>C NMR (75 MHz, [D<sub>8</sub>]THF): δ= 152.0, 151.9, 149.2, 143.2, 143.1, 142.2, 142.1, 142.0, 141.5, 141.1, 140.3, 140.1, 133.3, 132.5, 132.1, 131.1, 130.8, 129.8, 129.6, 129.6, 129.2, 129.0, 128.8, 128.8, 128.5, 128.3, 128.2, 128.1, 128.0, 126.8, 126.7, 126.5, 125.9, 125.8, 125.8, 124.6, 124.4, 124.3, 123.8, 123.4, 122.7, 122.0. HRMS (FAB/magnetic sector) m/z: [M]<sup>+</sup> Calcd. for C<sub>55</sub>H<sub>33</sub>Br, 772.1766; Found 772.1775.

**2,5'-Di([1,1':3',1''-terphenyl]-5'-yl)spiro[fluorene-9,15'-indeno[2,1-g]chrysenel] (TP-CS-TP).** Compd **5** (0.4 g, 0.52 mmol), compd **7** (0.22 g, 0.62 mmol), Pd(OAc)<sub>2</sub> (0.004 g, 0.018 mmol), and tricyclohexylphosphine (0.012 g, 0.043 mmol) were added to anhydrous THF (100 mL). Then, (Et)<sub>4</sub>NOH (20 wt%, 10 mL) was added to the reaction mixture at 50 °C. The mixture was refluxed for 3 h under nitrogen. After the reaction was complete, the reaction mixture was extracted with chloroform and water. The organic layer was dried with anhydrous MgSO<sub>4</sub> and filtered. The solution was evaporated. The product was isolated with silica gel column chromatography using chloroform : n-hexane (1:3) as the eluent to obtain a white solid (0.43 g, 90%). <sup>1</sup>H NMR (300 MHz, [D<sub>8</sub>]THF): δ= 9.21 (d, 1H), 9.10 (d, 1H), 8.92 (s, 1H), 8.55 (d, 1H), 8.28 (d, 1H), 8.17 (d, 1H), 7.99 (s, 1H), 7.88-7.80 (m, 7H), 7.77 (d, 4H), 7.64 (s, 1H), 7.53 (t, 6H), 7.44 (q, 5H), 7.35-7.23 (m, 7H), 7.20 (t, 4H), 7.00 (t, 2H), 6.70-6.64 (m, 2H), 6.53(d, 1H); <sup>13</sup>C NMR (75 MHz, [D<sub>8</sub>]THF): δ= 152.7, 150.5, 149.8, 143.2, 143.0, 142.8, 142.6, 142.5, 142.1, 142.0, 141.5, 141.1, 141.0, 140.2, 133.2, 132.4, 131.3, 130.7, 129.7, 129.5, 129.1, 128.8, 128.4, 128.2, 128.2, 128.0, 127.9, 126.7, 126.2, 125.8, 124.5, 124.2, 123.9, 123.6, 122.5, 122.2, 121.8. HRMS (FAB/magnetic sector) m/z: [M+H]<sup>+</sup> Calcd. for C<sub>73</sub>H<sub>47</sub>, 923.3633; Found, 923.3639. Anal. Calcd. for C<sub>73</sub>H<sub>46</sub>: C 94.98, H 5.02; Found: C 94.75, H 5.06.

## ASSOCIATED CONTENT

### Supporting Information

The Supporting Information is available free of charge on the ACS Publications website at DOI:

X-ray data for CS

UV-Vis, PL spectrum, X-ray data, TRPL, CV, TGA, DSC data, <sup>1</sup>H NMR, and <sup>13</sup>C NMR spectra.

## AUTHOR INFORMATION

### Corresponding Author

\* E-mail: jongpark@khu.ac.kr

### ORCID

Sang Hyuk Im: 0000-0001-7081-5959

Jongwook Park: 0000-0002-6797-5211

### Notes

The authors declare no competing financial interest.

## ACKNOWLEDGMENT

This research was supported by a grant from the Technology Development Program for Strategic Core Materials funded by the Ministry of Trade, Industry & Energy, Republic of Korea (Project No. 10047758). This research was supported by a grant from the Core Technology Development Program for the Commercialization of Functional Chemicals funded by the Ministry of Trade, Industry and Energy, Republic of Korea (Project No. 10060523). This research was supported by National R&D Program through the National Research Foundation of Korea(NRF) funded by the Ministry of Science & ICT (No.2017M3A7B4041699).

## REFERENCES

- (1) Guo, J.; Li, X. L.; Nie, H.; Luo, W.; Gan, S.; Hu, S.; Hu, R.; Qin, A.; Zhao, Z.; Su, S. J.; Tang, B. Z. *Adv. Funct. Mater.*, **2017**, *27*, 1606458.
- (2) Tseng, H. S.; Phan, H.; Luo, C.; Wang, M.; Perez, L. A.; Patel, S. N.; Ying, L.; Kramer, E. J.; Nguyen, T. Q.; Bazan, G. C.; Heeger, A. J. *Adv. Mater.*, **2014**, *26*, 2993-2998.
- (3) Wu, Q.; Zhao, D.; Yang, J.; Sharapov, V.; Cai, Z.; Li, L.; Zhang, N.; Neshchandin, A.; Chen, W.; Yu, L. *Chem. Mater.*, **2017**, *29*, 1127-1133.
- (4) (a) Lorente, A.; Pingel, P.; Liaptsis, G.; Krüger, H.; Janietz, S. *Org. Electron.*, **2017**, *41*, 91-99. (b) Li, J.; Han, X.; Bai, Q.; Shan, T.; Lu, P.; Ma, Y. *J. Polym. Sci. A Polym. Chem.*, **2017**, *55*, 707-715.
- (5) (a) Kim, S. K.; Yang, B.; Park, Y. I.; Ma, Y.; Lee, J. Y.; Kim, H. J.; Park, J. *Org. Electron.*, **2009**, *10*, 822-833. (b) Lee, H.; Kim, B.; Kim, S.; Kim, J.; Lee, J.; Shin, H.; Lee, J. H.; Park, J. *J. Mater. Chem. C*, **2014**, *2*, 4737-4747. (c) Lee, J.; Kim, B.; Kwon, J. E.; Kim, J.; Yokoyama, D.; Suzuki, K.; Nishimura, H.; Wakamiya, A.; Park, S. Y.; Park, J. *Chem. Commun.*, **2014**, *50*, 14145-14148. (d) Lee, H.; Jo, M.; Yang, G.; Jung, H.; Kang, S.; Park, J. *Dyes Pigm.* **2017**, *146*, 27-36.
- (6) (a) Kuma, H.; Hosokawa, C. *Sci. Techol. Adv. Mater.*, **2014**, *15*, 034201. (b) Zhao, Lei.; Wang, Shumeng.; Ding, Junqiao.; Wang, Lixiang. *Org. Electron.*, **2018**, *53*, 43-49. (c) Bai, Keyan.; Wang, Shumeng.; Zhao, Lei.; Ding, Junqiao.; Wang, Lixiang. *Polym. Chem.*, **2017**, *8*, 2182-2188. (d) Yu, Mingquan.; Wang, Shumeng.; Shao, Shiyang.; Ding, Junqiao.; Wang, Lixiang.; Jing, Xiabin.; Wang, Fosong. *J. Mater. Chem. C*, **2015**, *3*, 861-869.
- (7) (a) Kim, S.; Kim, B.; Lee, J.; Shin, H.; Park, Y. I.; Park, J. *Mater. Sci. Eng. R Rep.*, **2016**, *99*, 1-22. (b) Shin, H.; Jung, H.; Kim, B.; Lee, J.; Moon, J.; Kim J.; Park, J. *J. Mater. Chem. C*, **2016**, *4*, 3833-3842.
- (8) Huang, J.; Sun, N.; Dong, Y.; Tang, R.; Lu, P.; Cai, P.; Li, Q.; Ma, D.; Qin, J.; Li, Z. *Adv. Funct. Mater.*, **2013**, *23*, 2329-2337.
- (9) (a) Lei, T.; Luo, J.; Wang, L.; Ma, Y.; Wang, J.; Cao, Y.; Pei, J. *New. J. Chem.*, **2010**, *34*, 699-707. (b) Luo, J.; Zhou, Y.; Niu, Z. Q.; Zhou, Q. F.; Ma, Y.; Pei, J. *J. Am. Chem. Soc.*, **2007**, *129*, 11314-11315. (c) Liu, F.; Xie, L. H.; Tang, C.; Liang, J.; Chen, Q. Q.; Peng, B.; Wei, W.; Cao, Y.; Huang, W. *Org. Lett.*, **2009**, *11*, 3850-3853.
- (10) (a) Lee, J.; Park, J. *Org. Lett.*, **2015**, *17*, 3960-3963. (b) Park, S. H.; Jin, Y.; Kim, J. Y.; Kim, S. H.; Kim, J.; Suh, H.; Lee, K. *Adv. Funct. Mater.*, **2007**, *17*, 3063-3068. (c) Skoog, D. A.; West, D. M.; Holler, F. J.; Crouch, S. R. *Molecular Fluorescence Spectroscopy. Fundamentals of Analytical of Chemistry*, 8; Brooks/Cole: Cengage Learning, Belmont, CA, USA, 2004; pp 828.
- (11) Kim, E.; Koh, M.; Lim, B. J.; Kim, S. B. *J. Am. Chem. Soc.*, **2011**, *133*, 6642-6649
- (12) (a) Iannotta, S.; Toccolli, T.; Boschetti, A.; Scardi, P. *Synth. Met.*, **2001**, *122*, 221-223. (b) Ichino, Y.; Ni, J. P.; Ueda, Y.; Wang, D. K. *Synth. Met.*, **2001**, *116*, 223-227. (c) Cornil, J.; Beljonne, D.; Shuai, Z.; Hagler, T. W.; Campbell, I.; Bradley, D. D. C.; Brédas, J. L.; Spangler, C. W.; Müllen, K. *Chem. Phys. Lett.*, **1995**, *247*, 425-432.
- (13) Danel, K.; Huang, T. H.; Lin, J. T.; Tao, Y. T.; Chuen, C. H. *Chem. Mater.*, **2002**, *14*, 3860-3865
- (14) Park, Y.; Kim, S.; Lee, J. H.; Jung, D. H.; Wu, C. C.; Park, J. *Org. Electron.*, **2010**, *11*, 864-871.
- (15) (a) Bach, U.; Cloedt, K. D.; Spreitzer, H.; Grätzel, M. *Adv. Mater.*, **2000**, *12*, 1060-1036. (b) Salbeck, J.; Yu, N.; Bauer, J.; Weissörtel, F.; Bestgen, H. *Synth. Met.*, **1997**, *91*, 209-215.
- (16) O'Brien, D. F.; Burrows, P. E.; Forrest, S. R.; Koene, B. E.; Loy, D. E.; Thompson, M. E. *Adv. Mater.*, **1997**, *10*, 1108-1112.
- (17) Giebink, N. C.; Forrest, S. R. *Phys. Rev. B*, **2008**, *77*, 235215.

1 (18) Gaussian 09, Revision D.1, Frisch, M. J.; Trucks, G. W.; Schlegel, H. B.; Scuseria, G. E.; Robb, M. A.; Cheeseman, J. R.; Scalmani,  
2 G.; Barone, V.; Mennucci, B.; Petersson, G. A.; Nakatsuji, H.; Caricato, M.; Li, X.; Hratchian, H. P.; Izmaylov, A. F.; Bloino, J.; Zheng, G.;  
3 Sonnenberg, J. L.; Hada, M.; Ehara, M.; Toyota, K.; Fukuda, R.; Hasegawa, J.; Ishida, M.; Nakajima, T.; Honda, Y.; Kitao, O.; Nakai,  
4 H.; Vreven, T.; Montgomery, J. A., Jr.; Peralta, J. E.; Ogliaro, F.; Bearpark, M.; Heyd, J. J.; Brothers, E.; Kudin, K. N.; Staroverov, V.  
5 N.; Kobayashi, R.; Normand, J.; Raghavachari, K.; Rendell, A.; Burant, J. C.; Iyengar, S. S.; Tomasi, J.; Cossi, M.; Rega, N.; Millam, J.  
6 M.; Klene, M.; Knox, J. E.; Cross, J. B.; Bakken, V.; Adamo, C.; Jaramillo, J.; Gomperts, R.; Stratmann, R. E.; Yazyev, O.; Austin, A.  
7 J.; Cammi, R.; Pomelli, C.; Ochterski, J. W.; Martin, R. L.; Morokuma, K.; Zakrzewski, V. G.; Voth, G. A.; Salvador, P.; Dannenberg, J.  
8 J.; Dapprich, S.; Daniels, A. D.; Farkas, Ö.; Foresman, J. B.; Ortiz, J.  
9 V.; Cioslowski, J.; Fox, D. J. Gaussian, Inc., Wallingford CT, **2009**.

10 (19) Sheldrick, G. M. *Acta Cryst.*, **2008**, A64, 112.

11 (20) Kim, B.; Park, Y.; Lee, J.; Yokoyama, D.; Lee, J. H.; Kido, J.;  
12 Park, J. *J. Mater. Chem. C*, **2013**, 1, 432-440.  
13  
14  
15  
16  
17  
18  
19  
20  
21  
22  
23  
24  
25  
26  
27  
28  
29  
30  
31  
32  
33  
34  
35  
36  
37  
38  
39  
40  
41  
42  
43  
44  
45  
46  
47  
48  
49  
50  
51  
52  
53  
54  
55  
56  
57  
58  
59  
60